Kullback-Leibler divergence measure of intermittency: Application to turbulence

Carlos Granero-Belinchón, Stéphane G. Roux, and Nicolas B. Garnier*
Univ Lyon, Ens de Lyon, Univ Claude Bernard, CNRS UMR 5672, Laboratoire de Physique, F-69342 Lyon, France

(Received 19 July 2017; revised manuscript received 27 November 2017; published 16 January 2018)

For generic systems exhibiting power law behaviors, and hence multiscale dependencies, we propose a simple tool to analyze multifractality and intermittency, after noticing that these concepts are directly related to the deformation of a probability density function from Gaussian at large scales to non-Gaussian at smaller scales. Our framework is based on information theory and uses Shannon entropy and Kullback-Leibler divergence. We provide an extensive application to three-dimensional fully developed turbulence, seen here as a paradigmatic complex system where intermittency was historically defined and the concepts of scale invariance and multifractality were extensively studied and benchmarked. We compute our quantity on experimental Eulerian velocity measurements, as well as on synthetic processes and phenomenological models of fluid turbulence. Our approach is very general and does not require any underlying model of the system, although it can probe the relevance of such a model.

DOI: 10.1103/PhysRevE.97.013107

I. INTRODUCTION

Complex systems are omnipresent in day life and as a consequence in many scientific fields. These are as various as Internet traffic [1,2], human genome exploration [3], geography [4], financial markets [5,6], etc. In recent years, increasing computational power and storage has fueled interest in accumulating and analyzing large amounts of data, and hence in developing tools to characterize systems where traditional methods are not relevant. Real-world systems are most commonly nonlinear, and their complexity is difficult to model. Hence, any pertinent tool must be able to probe nonlinear correlations and should preferably be nonparametric.

A very common characteristic of such systems is the occurrence of quantities that exhibit a power spectral density (PSD) with a power law, indicating that multiple scales are present, in a continuous range. In addition, probability density functions (PDFs) are most commonly non-Gaussian, suggesting that nonlinear interactions are at work. When one defines and then measures a global or local quantity which has both a power law power spectrum and a non-Gaussian PDF, this quantity is usually shown to have a fractal nature, with a deformation of its PDF when the scale varies. Again, very few tools exist to probe such systems correctly. We propose here a measure of the evolution between Gaussian and non-Gaussian PDF. Another wide class of problems considers a global quantity defined as the sum or integral, e.g., over space or over time, of a local quantity that has non-Gaussian statistics. Estimating or predicting the statistics of the global quantity is usually not easy, because of, e.g., long-range interactions that lead to long-range correlations. Nevertheless, for large integration scales, larger than any possible correlation scale, large deviation theory should reduce to the central limit theorem and Gaussian statistics are expected. We also aim at quantifying these transformations of the PDFs.

One paradigm of multiscale complex systems is fluid turbulence, for which many theoretical and phenomenological developments have been proposed to describe very complex behaviors such as energy cascade and intermittency.

Kolmogorov's 1941 theory (K41) [7–9] provided a powerful framework to describe fully developed turbulence, and in particular to characterize its statistical properties. Considering, for example, Eulerian longitudinal velocity increments $\delta_l v$ at scale l, K41 theory states that the p-order structure function $S_p(l) \equiv \langle (\delta_l v)^p \rangle$ behaves, for any positive integer p, as a power law of the scale l,

$$S_p(l) \propto l^{\zeta(p)}, \tag{1}$$

in the inertial range $\eta \ll l \ll L$, where L and η are the integral and Kolmogorov scales. The scaling exponent $\zeta(p)$ depends on the order p, and K41 theory, assuming homogeneity and isotropy at the small scales of the flow, predicts a linear behavior of the scaling exponents as $\zeta(p) = p/3$. Using the relation between the kinetic energy and the second order structure function $S_2(l)$, this implies the famous 5/3 law for the distribution of kinetic energy in the inertial range. The existence of the energy cascade from larger scales to smaller ones has been shown by Kolmogorov to be related to the 4/5 law, which imposes the value of the third order structure function $S_3(l)$.

Although very satisfying at first, this predicted linear behavior of the scaling exponents was later rejected by dedicated experiments [10]. To describe the observed deviations, Kolmogorov and Oboukhov relaxed some of the K41 hypotheses: in particular, they assumed a spatially intermittent distribution of the local dissipation rate [11,12]. This led to the KO62 theory and the definition of intermittency in turbulence: the scaling exponents $\zeta(p)$ do not depend linearly in p (see Fig. 3).

Intermittency was later related to the multifractal description of turbulence as stated by Frisch and Parisi [13]. It is now recognized that the PDF of the Eulerian velocity increments continuously deforms from Gaussian at large scales $l \gtrsim L$ to strongly non-Gaussian at smaller scales, and we use this

*nicolas.garnier@ens-lyon.fr

consequence as an equivalent, but more practical, definition of intermittency.

The deformation of the PDF can be quantified by the evolution of its flatness [14], measured as the normalized kurtosis of the distribution: $\langle(\delta_l v)^4\rangle/\langle(\delta_l v)^2\rangle^2 = S_4(l)/S_2(l)^2$. At larger scales, about or above the integral scale L, the PDF of the velocity increments is almost Gaussian and has a flatness very close to three. For smaller and smaller scales, the PDF is less and less Gaussian as the PDF of the normalized increments becomes wider and wider; therefore the flatness increases. Fine evolutions of the PDF, and hence intermittency, have been studied with the flatness, such as a rapid increase of intermittency when the scale is reduced down or below the Kolmogorov dissipative scale [15]. S_2 evolves according to the 2/3 law predicted by K41 theory, so, the kurtosis only involves one higher-order structure function, namely, S_4, and as such it does not describe the deviation of all the scaling exponents $\zeta(p)$ from their linear behavior in p. This is why we propose in this article a measure of intermittency that involves all structure functions.

Shannon founded information theory in 1948 and introduced entropy as a measure of the total information of a process [16]. Since then, information theory has been widely used in very different fields: biomedical science [17–19], physics of fluids [20–22], thermodynamics [23], and others. Shannon entropy is a functional of the PDF of the process, and as such it depends on all the moments of the distribution; see Sec. II.

We propose a measure of intermittency, interpreted as the deformation of a PDF which is Gaussian at large scales. To do so, we consider the Kullback-Leibler (KL) divergence [24] between the PDF and the Gaussian PDF defined with the same standard deviation. The KL divergence has been scarcely used in the field of turbulence, usually as an *a posteriori* quantitative comparison of theoretically predicted PDFs with experimental [25] or approximated ones [26]. We compute this quantity for Eulerian velocity increments, in order to measure intermittency in turbulence. We do so in a wide range of scales so that we can observe how this measure of intermittency behaves in all domains of fluid turbulence. By comparing the PDF, defined by all its moments, and the Gaussian approximation of this PDF, defined by the second order moment only, we measure not only the growth of the pth order moment with respect to the variance, but also the evolution of all the moments with respect to the variance; i.e., we exhaustively characterize the deformation of the PDF. Measuring the intermittency with a KL divergence provides a generalization of measures such as flatness ($p = 4$), hyperflatness ($p = 6$), etc.

Although we propose to study turbulence as an application of our framework, our definitions are very general and require only a signal to probe intermittency. Our approach does not require any *a priori* knowledge of the signal or any underlying model of the system that produced the signal. As such, it can prove a very powerful tool to analyze complex systems exhibiting power law behaviors or multiscale dependencies.

This paper is organized as follows. In Sec. II we define our information theoretical measure of intermittency that involves Shanon entropy and a well-chosen Kullback-Leibler divergence. In Sec. III we compute this quantity for experimental measurements of the Eulerian velocity field in several setups and several Reynolds numbers. We then turn in Sec. IV to some phenomenological modelings in order to better understand and describe our observations.

II. DEFINITIONS

A. Entropy and KL divergence from Gaussianity

Shannon entropy, $H(X)$, of a process X of PDF $p(x)$, is the total information that defines the process [16]. It depends on all the moments of the PDF $p(x)$ except the first order one:

$$H(X) = -\int_{\mathbb{R}} p(x)\ln p(x)\,dx. \tag{2}$$

We know that a Gaussian process, X_G, is uniquely defined by the prescription of its mean, variance, and two-point correlation function. Therefore, its Shannon entropy depends only on its variance $\sigma^2_{X_G}$, and we have the analytical expression of the entropy $H(X_G)$ of a Gaussian process X_G:

$$H(X_{\mathrm{G}}) = \tfrac{1}{2}\ln\left(2\pi e\sigma^2_{X_{\mathrm{G}}}\right). \tag{3}$$

For a generic process X which is *a priori* non-Gaussian and has the variance σ^2_X, we define the "entropy under Gaussian hypothesis" $H_{\mathrm{G}}(X)$ as the entropy that one would get assuming the process is Gaussian and using Eq. (3):

$$H_{\mathrm{G}}(X) = \tfrac{1}{2}\ln\left(2\pi e\sigma^2_X\right), \tag{4}$$

where σ_{X} is the standard deviation of the generic process X. So the "entropy under Gaussian hypothesis" of X is a measure of the entropy of a Gaussian PDF with the same standard deviation as the real PDF of X. If X is Gaussian, obviously $H_{\mathrm{G}}(X_{\mathrm{G}}) = H(X_{\mathrm{G}})$.

For any process X with probability density function $p(x)$, we can measure the difference between the "real" PDF $p(x)$ of X and the Gaussian approximation $p_{\mathrm{G}}(x)$ using the Kullback-Leibler divergence [24]:

$$\mathcal{K}_{p||p_{\mathrm{G}}}(X) = \int_{\mathbb{R}} p(x)\ln\left[\frac{p(x)}{p_{\mathrm{G}}(x)}\right]dx. \tag{5}$$

Using the definitions of $H(X)$ and $H_G(X)$, we have

$$\mathcal{K}_{p||p_{\mathrm{G}}}(X) = H_{\mathrm{G}}(X) - H(X) \geqslant 0. \tag{6}$$

$\mathcal{K}_{p||p_{\mathrm{G}}}(X)$ is a measure of the distance from Gaussianity of the process X, i.e., the distance between the PDF $p(x)$ of X and a Gaussian PDF $p_{\mathrm{G}}(x)$ which has the same standard deviation. The maximum entropy principle [27,28] states that for a given standard deviation, the Gaussian PDF maximizes the entropy; see also Ref. [29]. So this distance is also a comparison between the total information needed to define the process and the total information defining the most ambiguous process with the same standard deviation. The maximization of the entropy for the Gaussian case ensures that the difference $H_{\mathrm{G}}(X) - H(X)$ is always positive, as expected for a KL divergence and vanishes only when X has a Gaussian distribution.

B. Distance from Gaussianity across scales

We analyze the process X at scale τ by studying its increments of size τ:

$$\delta_\tau X(t) = X(t+\tau) - X(t). \tag{7}$$

We note $D_\tau(X)$, the KL divergence $\mathcal{K}_{p||p_G}(\delta_\tau X)$ which measures the distance from Gaussianity of the increments at scale τ of a process X:

$$D_\tau(X) = \mathcal{K}_{p||p_G}(\delta_\tau X) = H_G(\delta_\tau X) - H(\delta_\tau X). \quad (8)$$

This quantity measures the deformation of the PDF of the increment as a function of the size τ of the increment: it quantifies the evolution of the shape of the PDF, which depends on all the moments of the process, except its mean.

Indeed, at each scale τ, the increment $\delta_\tau X$ has a different standard deviation. The larger the scale τ, the higher the standard deviation. So changing τ changes quantitatively the entropies $H(\delta_\tau X)$ and $H_G(\delta_\tau X)$, which both depend strongly on the standard deviation. Subtracting the two entropies eliminates most of this quantitative variation because the standard deviation is by construction the same in both expressions $H_G(\delta_\tau X)$ and $H(\delta_\tau X)$. $D_\tau(X)$ thus measures only more subtle and delicate evolutions of the shape of the PDF than the trivial rescaling induced by the standard deviation.

In the specific case of turbulence, the PDFs of the increments of size equal or larger than the integral scale L are almost Gaussian. As a consequence, we expect that the distance from Gaussianity $D_\tau(X)$ tends to zero when τ approaches the integral scale. Conversely, it is expected to increase in the inertial range down to the dissipative scale where it should increase (even) faster [15]. Our distance from Gaussianity should therefore be able to probe intermittency of turbulence by measuring the deformation of the PDF of velocity increments.

C. Methodology

To compute the Shannon entropy H from experimental time series, one can first estimate the PDF by constructing the histogram and can then use Eq. (2), but this estimation procedure strongly depends on the size of the bins [30]. In order to compute accurately H from experimental data, we use instead a nearest neighbor estimator described by Kozachenko and Leonenko [31,32]. The only parameter used in this algorithm is the number of neighbors k involved in the nearest neighbors search. We chose the usual value $k = 5$ which is large enough to estimate the Shannon entropy correctly within a reasonable computational time.

Following Theiler [33], we subsample the data in order to remove spurious correlation effects: when computing the entropy of $\delta_\tau X(t)$, we retain only data points separated in time by a delay time $\tau_{\max}$, defined as the size of the largest increment that we compute. This prescription has two benefits. First, two successive points of the subsampled data set are uncorrelated, because the increments of size τ are typically correlated over a time $\tau \leqslant \tau_{\max}$. Second, the number N of points used in the computation of the entropy of $\delta_\tau X$ is independent of τ, so the bias due to finite size effects is constant when τ is varied. To compute the entropy under Gaussian hypothesis H_G, we estimate the standard deviation of the process and then use Eq. (3).

In the remainder of this article, all quantities are computed using $N = 512$ points, $\tau_{\max} = 4096$, so signals with a total of $N\tau_{\max} = 2^{21}$ points. We also average our results over independent realizations, in order to compute the standard deviation of the quantities and provide error bars to the estimations. We use 12 realizations for experimental signals and eight realizations for synthetic processes.

In following sections we analyze the evolution of the PDF along the scales for a longitudinal turbulent velocity signal. We compare the obtained results with some synthetic and theoretical models of turbulence.

III. TURBULENCE

A. Experimental signals

We analyze two different sets of experimental turbulent data, in order to show the ability of our measures to grasp inherent properties of turbulence.

The first system consists of a temporal measurement of the longitudinal velocity (V) at one location in a grid turbulence setup in the wind tunnel of ONERA at Modane [34]. The Taylor-scale based Reynolds number $\mathbb{R}_\lambda$ is about 2500, with a turbulence intensity about 8%. The inertial region spans approximately three decades. The sampling frequency is $f_s =$ 25 kHz, and the mean velocity of the wind in the tunnel is $\langle v \rangle = 20.5$ m/s. The probability density function of the data is almost Gaussian although there is some visible asymmetry: the skewness is about 0.175 ± 0.001.

The second system is a set of temporal velocity measures at different Reynolds numbers in a jet turbulence experiment with helium [35]. The Taylor-scale-based Reynolds number $\mathbb{R}_\lambda$ is respectively 89, 208, 463, 703, 929, with a turbulence intensity about 23%.

Using the Taylor hypothesis [14] and the mean velocity $\langle v \rangle$ of the flow, we interpret these time series as the spatial evolution of the longitudinal velocity. The time scale τ and the spatial scale l are related by $l = \langle v \rangle \tau$. We note the integral time scale T and the integral spatial scale L, and we have $L = \langle v \rangle T$. We present all our results as functions of the ratio $\tau/T = l/L$ between the scale of the increment and the integral scale.

B. Results

In Fig. 1, we present the analysis of the Modane experimental velocity data. In the left column, we report the classical viewpoint and compare it to the information theory viewpoint in the right column.

We first plot the power spectrum of the velocity signal V as a function of the inverse frequency $1/f = \tau$ in Fig. 1(a): it shows the distribution of energy across scales following the well-known 5/3 Kolmogorov law. In order to measure the deformation of the shape of the PDF of the velocity increment when the scale τ is varied, we follow Frisch [14], and compute the flatness as the kurtosis $\langle (\delta_\tau v)^4 \rangle / \langle (\delta_\tau v)^2 \rangle^2$ of the velocity increments normalized by three, the kurtosis of a Gaussian PDF. Results are reported in 1(b). For $\tau \gtrsim T$, i.e., $l \gtrsim L$, the flatness has the value expected for a Gaussian PDF. Reducing τ, the flatness increases. When τ is smaller than the dissipative scale [15], the increase of the flatness is sharper. Three different regions can be distinguished in both figures: integral, inertial, and dissipative.

The right column of Fig. 1 is devoted to the information theory viewpoint on the same characteristics of turbulence. We first plot the entropy of the increments in Fig. 1(c) and

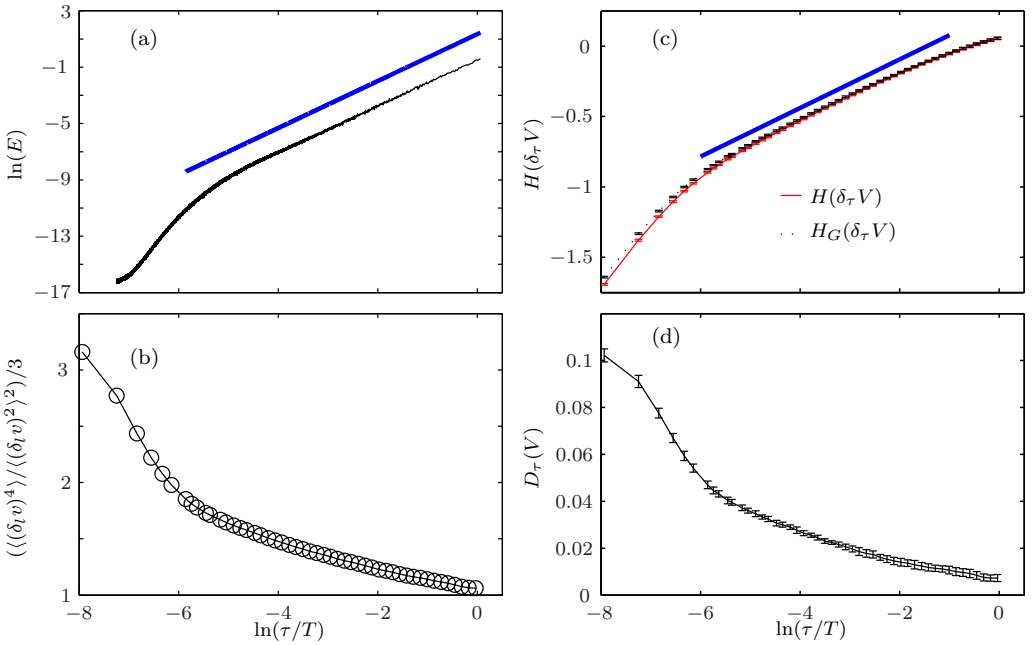

FIG. 1. (a) Power spectrum, (b) flatness, (c) entropies, and (d) KL distance from Gaussianity, for the Modane experimental data, as functions of $\ln(\tau/T) = \ln(l/L)$, the logarithm of scale normalized by the integral scale. In (a) and (c), the straight lines indicate the theoretical scaling in the inertial region predicted by Kolmogorov K41 theory.

compare it with the PSD in Fig. 1(a). We then plot $D_\tau(V)$ in Fig. 1(d) and compare its behavior in τ with the flatness.

In Fig. 1(c) we see that the entropy of the increments $[H(\delta_\tau V)]$ increases with τ. The larger the scale, the higher the total Shannon information needed to completely characterize the increment. We can distinguish three different ranges with different dependence of the entropy on the scale. For the large scales, larger than the integral scale, the entropy reaches its highest value and is then constant. So the most disorganized or complex scales, the ones requiring more information to be completely characterized, are the scales in the integral domain. Within this region, the characterization of the scale does not require more entropy when the size of the increment increases. A linear behavior of the entropy in $\ln(\tau/T)$ is found in the inertial region, $\tau \in [10,400]$. The complexity of the scales, as measured by $H(\delta_\tau V)$, decreases linearly in $\ln(\tau/T)$ between the integral and the Kolmogorov scales. For the smallest scales, below the Kolmogorov scale, which we can measure at $\ln(\tau/T) \approx -5$, we observe a steeper decrease of the disorganization when the scale decreases. So, using the entropy of the increments, we are able to recover the three different regions. Moreover, we can state that $H(\delta_\tau V)$ increases from the smallest scale to the integral scale and then remains constant. In addition, the evolution of $H(\delta_\tau V)$ in the inertial region is linear in $\ln(\tau/T)$.

Both entropies $H(\delta_\tau V)$ and $H_G(\delta_\tau V)$ in Fig. 1(c) are indistinguishable in the integral domain. The distance between them starts to increase when we enter the inertial region. In Fig. 1(d), we plot the difference between these two entropies, which, according to Eq. (8) is the distance from Gaussianity $D_\tau(V)$. Starting from zero at scales larger than the integral one, it increases when the scale decreases. The vanishing of $D_\tau(V)$ for largest scales implies that the PDF of the velocity increments is almost Gaussian, which is the expected behavior in turbulence at scales equal to or larger than the integral scale. Below this integral scale the PDF starts to deform and becomes less and less Gaussian when the scale decreases. The evolution of $D_\tau(V)$ is almost linear between the integral and the Kolmogorov scales. Finally, in the dissipative range, we observe an abrupt deformation of the PDF, in perfect agreement with the rapid increase of the flatness in Fig. 1(b). [15] The distance from Gaussianity $D_\tau(V)$ across scales τ is a measure of the deformation of the PDF of the turbulent velocity increments and, as such, a measure of the intermittency.

In the four subplots of Fig. 1, the three different domains of turbulence are distinguishable: integral, inertial, and dissipative. Figure 1(c) allows us to interpret these three domains in terms of organization and complexity of velocity increments. Figure 1(d) shows that the KL divergence allows us to quantify the evolution of intermittency among scales τ. We not only recover the three different ranges with our measures based on information theory, but the qualitative behavior of intermittency in each domain is also in perfect agreement with previous studies. Moreover, our measure of intermittency doesn't depend on a specific ratio between selected moments of the PDFs like the kurtosis. $D_\tau(V)$ takes into account all the moments defining the PDFs: this makes our KL distance from Gaussianity across scales a good candidate for a quantitative measure of intermittency.

We have compiled information theory results for all experimental signals in Fig. 2, in order to study the influence of the Reynolds number. The entropy as a function of the scale is reported in Fig. 2(a); we observe how the size of the inertial range varies with the Reynolds number, with the Kolmogorov scale increasing when the Reynolds number decreases. This classical behavior of the Kolmogorov scale is also recovered with the KL divergence, represented in Fig. 2(b). The steeper slope, which indicates the dissipative domain, appears at higher

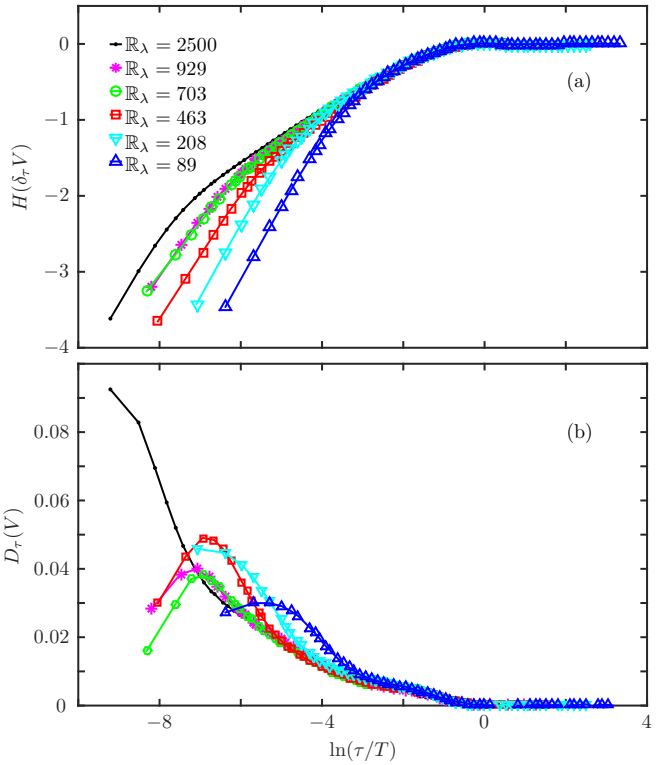

FIG. 2. (a) Entropy $H(\delta_\tau V)$ of the Eulerian velocity increments as a function of $\ln(\tau/T) = \ln(l/L)$. (b) KL divergence $D_\tau(V) = H_G(\delta_\tau V) - H(\delta_\tau V)$. Different experimental signals with various Reynolds numbers have been used.

scales when the Reynolds number is lower; we recover the dependence of the Kolmogorov scales with the Reynolds number.

The behaviors of both the entropy and the distance from Gaussianity are qualitatively the same for different experimental setups and for any Reynolds number. The dependence of the entropy $H(\delta_\tau V)$ of the increments is, at first order, in agreement with the K41 theory: we recover the scaling law in the inertial domain [36]. The KL divergence $D_\tau(V)$ then enlightens the deformation of the PDF across scales, which is qualitatively compatible with the K062 theory and hence the intermittency in turbulence.

IV. MODELING

In order to get some insight on the quantitative results obtained with our Kullback-Leibler divergence D_τ, we now turn to some theoretical descriptions of the inertial domain of fully developed turbulence.

First, we study different processes. Among the simplest, popular, and most important is fractional Brownian motion (fBm) [7,37], which, as a monofractal process, doesn't display intermittency. We also explore multifractal processes that exhibit intermittency: multifractal random walk (MRW) [38,39] and random wavelet cascade (RWC) with log-normal [39,40] or log-Poisson distribution of multipliers [39–41]. We then examine the propagator formalism [42], a phenomenological model that provides an analytical expression of the PDF of the velocity increments [43].

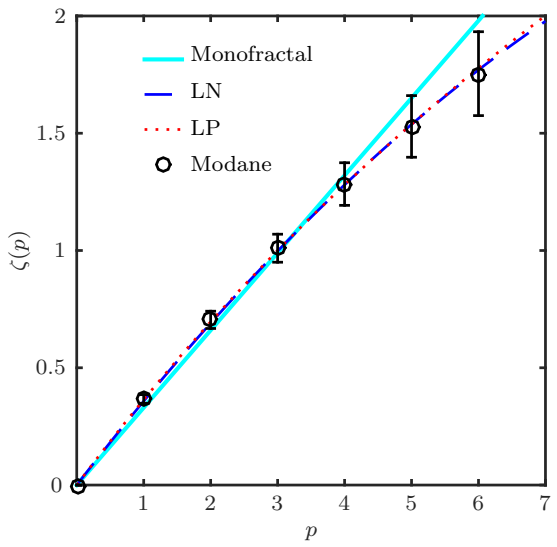

FIG. 3. Scaling exponents $\zeta(p)$ versus order p for three different models of turbulence in the inertial domain, together with an experimental Eulerian velocity measure (Modane, black symbols). Models are monofractal fractional Brownian motion (cyan, continuous straight line), multifractal log-normal (blue, dashed line), and multifractal log-Poisson (red, dotted line).

A. Description of turbulence

We briefly introduce the models that we use. All are characterized by the set of their scaling exponents, $\zeta(p)$, as they appear in Eq. (1). One of the very few exact results of Kolmogorov's framework is the 4/5 law, which imposes $\zeta(3) = 1$; this should be respected by any model or process representing turbulence; see Fig. 3. A linear behavior of the scaling exponents with p characterizes a monofractal process. On the other hand, a nonlinear behavior reveals multifractality; see Fig. 3.

From these scaling exponents, one can define the log-cumulants from the following Taylor expansion [44]:

$$\zeta(p) = c_1 p - c_2 \frac{p^2}{2!} + c_3 \frac{p^3}{3!} \cdots . \tag{9}$$

So the existence of nonzero log-cumulants c_p of order $p \geqslant 2$ indicates the multifractal nature of a process.

By taking the Legendre transform of the scaling exponents we estimate the singularity spectrum of the process [13]:

$$\mathcal{D}(h) = \min_p [ph - \zeta(p)], \tag{10}$$

where h is called the Hölder exponent and describes the local regularity of the signal. The singularity spectrum $\mathcal{D}(h)$ is related to the probability of finding the Hölder exponent h.

For a monofractal process there is only one possible value for the Hölder exponent h, which is notated $\mathcal{H}$, the Hurst exponent. The scaling exponent are linear in p (see Fig. 3): $\zeta(p) = \mathcal{H}p$, so only the first log-cumulant c_1 is nonzero: $c_1 = \mathcal{H}$. In that case, the scale invariance implies the following relation between the probability distributions $p_{\delta_\tau X}$ and $p_{\delta_{\tau_0} X}$ of the increments of scales τ and τ_0:

$$p_{\delta_\tau X}(\delta_\tau X) = \left(\frac{\tau_0}{\tau}\right)^{\mathcal{H}} p_{\delta_{\tau_0} X}\left[\left(\frac{\tau_0}{\tau}\right)^{\mathcal{H}} \delta_\tau X\right],$$

so

$$H(\delta_\tau X) = H(\delta_{\tau_0} X) + \mathcal{H}\ln(\tau/\tau_0). \tag{11}$$

This relation is valid for all couples of scales (τ,τ_0), and although there is no integral scale T in a monofractal description, we further note the reference scale $\tau_0 = T$. Following K41, we set $\mathcal{H} = c_1 = 1/3$ to model turbulence, although this is not very satisfying for larger p; see Fig. 3.

Intermittent log-normal model for turbulence was introduced by Kolmogorov and Oboukhov in 1962. It was the first intermittent model of turbulence, with the following scaling exponents: $\zeta(p) = c_1 p - c_2 \frac{p^2}{2}$.

The nonlinear dependence of the scaling exponents in p indicates the multifractal nature of the model, which is quantified by c_2. All log-cumulants c_p of order $p \geqslant 2$ are zero. Its singularity spectrum is

$$\mathcal{D}(h) = 1 - \frac{(h-c_1)^2}{2c_2}. \tag{12}$$

This multifractal process offers a satisfying representation of the scaling exponents of turbulence for $c_2 = 0.025$ and $c_1 = 1/3 + 3c_2/2 = 0.371$ (see Fig. 3).

The intermittent log-Poisson model was introduced by She and Leveque [41]. This heuristic model leads to scaling exponents of the form $\zeta(p) = -\gamma p - \lambda(\beta^p - 1)$. It has later been interpreted as a log-Poisson model with a singularity spectrum

$$\mathcal{D}(h) = 1 - \lambda + \frac{h-\gamma}{\ln(\beta)}\left\{\ln\left[\frac{h-\gamma}{-\lambda\ln(\beta)}\right] - 1\right\}. \tag{13}$$

The corresponding log-cumulants are

$$c_1 = \gamma + \lambda\ln(\beta), \tag{14}$$

$$c_m = \lambda\ln(\beta)^m, \quad m \geqslant 2. \tag{15}$$

This model imposes $\lambda = 2$, $\beta = (\frac{2}{3})^{(1/3)}$ and $\gamma = -1/9$ [41], and it describes the scaling exponents $\zeta(p)$ as satisfyingly as the log-normal model does (see Fig. 3).

B. Synthetic processes

We now briefly present the different processes that we numerically generated, according to the above prescriptions.

Fractional Brownian motion is the only scale-invariant process with Gaussian statistics and stationary increments. This monofractal process was introduced by Kolmogorov [7] and studied by Mandelbrot [37].

The Hurst exponent $\mathcal{H} = 1/3$ and σ_0 (the variance at $t = 0$) define completely the process. The power spectrum of fractional Brownian motion exhibits a 5/3 scaling, identical to the one of the energy in the inertial region of turbulence, in agreement with K41 [7]. We use the procedure presented by Helgason to synthesize fBm [45].

Log-normal multifractal processes: We use two different synthetic processes with log-normal statistics: a RWC [39,40] and a MRW [38]. Multifractality requires the existence of an integral scale T, from or towards which the PDF evolves. For both processes, we impose the integral scale T to be equal to the size of the signal.

TABLE I. The first three lines indicate the values of parameters [c_1 and c_2 and hence $\zeta(2)$] used in the generation. Estimates $\hat{c}_1$, $\hat{c}_2$, and $\hat{\zeta}(2)$ are obtained by classical multifractal analysis. The last line reports the slopes $\Delta_{\ln(\tau)} H_G(\delta_\tau X)$ of the entropy $H_G(\delta_\tau X)$ as a function of $\ln(\tau/T)$, for the four different models, which according to Eq. (16) provides another estimate of $\zeta(2)/2$.

	fBm	MRW	log-N	log-P
c_1	1/3	0.371	0.371	0.381
c_2	0	0.025	0.025	0.036
$\zeta(2)/2$	1/3	0.345	0.345	0.345
$\hat{c}_1$	0.333	0.42	0.372	0.382
$\hat{c}_2$	$1e^{-4}$	0.038	0.026	0.035
$\hat{\zeta}(2)/2$	0.332	0.363	0.353	0.356
$\Delta_{\ln(\tau)} H_G(\delta_\tau X)$	0.33 ± 0.01	0.37 ± 0.01	0.35 ± 0.01	0.35 ± 0.01

Log-Poisson multifractal process: We use a RWC with log-Poisson statistics [40]. Again, our synthesis fixes the integral scale T to the size of the generated signal.

Classical multifractal analysis offers a way to estimate the log-cumulants c_1 and c_2, but fails to estimate c_3 and higher order log-cumulants. It can therefore be interpreted as projecting the different models onto their log-normal approximation, with varying (c_1,c_2). For example, the multifractal analysis of a realistic log-Poisson model of turbulence leads the values given in Table I, and no additional higher order log-cumulant. As a consequence, such an analysis is not able to discriminate which process, log-normal or log-Poisson, better represents turbulence. For this reason, we compute in the next section the KL divergence D_τ which takes into account all moments of the PDF of increments, and hence higher order log-cumulants [46], in order to obtain a finer analysis of the inertial domain of turbulence.

C. Results

In Fig. 4(a) we plot for the four synthetic signals the entropy $H(\delta_\tau X)$ as a function of $\ln(\tau/T)$, the logarithm of the scale. We also plot the entropy under Gaussian hypothesis, $H_G(\delta_\tau X)$, but it is indistinguishable from $H(\delta_\tau X)$.

For any process, the entropy under Gaussian hypothesis H_G is computed using Eq. (4). It involves the second order moment $S_2(\tau)$ only, which we express using Eq. (1) as

$$S_2(\tau) = \sigma_\tau^2 = \sigma_T^2\left(\frac{\tau}{T}\right)^{\zeta(2)}.$$

We then obtain the dependence of H_G on the scale τ:

$$H_G(\delta_\tau X) = H_G(\delta_T X) + \frac{\zeta(2)}{2}\ln(\tau/T). \tag{16}$$

In Fig. 4(a), we observe that the slope of the curves, which should be $\frac{\zeta(2)}{2}$ is very similar for all processes: we report in Table I the different values we measured and compare them to the prescribed value (1/3 for fBM and 0.345 for all three multifractal processes). The distribution of information along the scales for the four different models is in agreement with the prescribed Kolmogorov K41 scaling [36].

Up to this point, looking at the entropies, the four models cannot be distinguished in the inertial domain. In Fig. 4(b) we plot the Kullback-Leibler divergence $D_\tau(X)$ as a function of

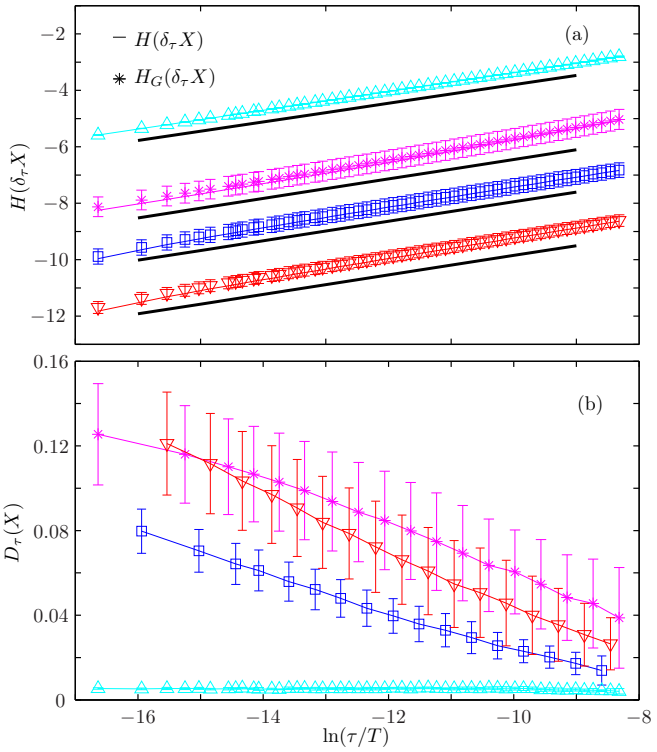

FIG. 4. (a) Entropy H (continuous curve) and entropy under Gaussian hypothesis H_G (symbols) for mono- and multifractal processes. Black lines represent the theoretical slope (1/3) for information expected for turbulence within K41 theory. (b) Distance $D_\tau(X) = H_G(\delta_\tau X) - H(\delta_\tau X)$ from Gaussianity. Four different models are used: fBm (cyan △), MRW (magenta ∗), log-normal RWC (blue □), and log-Poisson RWC (▽ red).

$\ln(\tau/T) = \ln(l/L)$, for scales ranging from $\tau/T = 1/2^{24}$ to $\tau/T = 4096/2^{24}$ where the integral scale is $T = 2^{24}$.

For a monofractal process, the entropy is given by Eq. (11), and the entropy under Gaussian hypothesis is given by Eq. (16) with $\mathcal{H} = \zeta(2)/2$, so $D_\tau(X) = H_G(\delta_\tau X) - H(\delta_\tau X)$ is constant and does not depend on the scale τ. If the monofractal process has Gaussian statistics, which defines the fBm, $D_\tau(X) = 0$ by construction. Looking at Fig. 4(b), D_τ for the fBm is not exactly zero; this is due to the bias in the estimation of $H(\delta_\tau X)$ and $H_G(\delta_\tau X)$. This bias is constant across scales, because our procedure was built to use a constant number of points in the range of τ we use.

For the three multifractal processes, $D_\tau(X)$ decreases monotonically when τ increases and tends to zero when the scale tends to the integral scale. So in the three multifractal models, the PDF of the increments deforms into a Gaussian PDF when approaching the integral scale. Moreover, in Fig. 4(b) we observe that the three processes, which indeed have different statistics, do not converge to zero in the same way. The distance from Gaussianity D_τ, by involving all the moments of the probability distributions, is able to reveal fine differences between processes.

The synthetic processes used above are good representations of the inertial range only. They do not properly take into account either the dissipative or the integral scales. Nevertheless, the synthesis imposes an effective integral scale

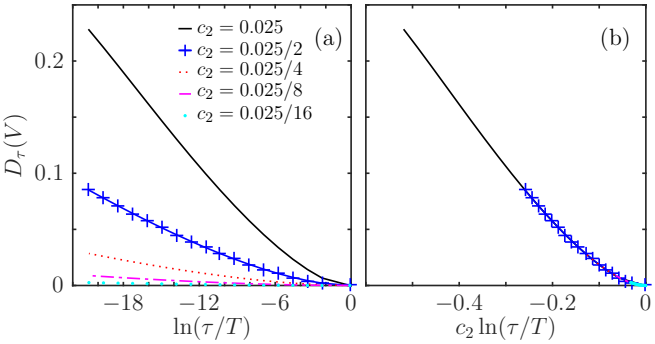

FIG. 5. Kullback-Leibler divergence D_τ for the log-normal propagator model, for varying values of the log-cumulant c_2, as a function of $\ln(\tau/T) = \ln(l/L)$ (a) or as a function of $c_2 \ln(\tau/T)$ (b).

that corresponds to the size of the generated signal. In order to study more precisely the deformation of the PDFs at large scale, we now turn to descriptions that explicitly involve the integral scale.

D. Phenomenological model: The propagator formalism

First introduced by Castaing [42], the propagator formalism describes the statistics of the Eulerian velocity increment $\delta_l v$ as identical, in the probabilistic sense, to the statistics of the product of two random variables: the large-scale fluctuations $\sigma_L \delta$ and the propagator $(l/L)^h$. The large-scale fluctuations are supposed Gaussian, with standard deviation σ_L, and δ is therefore a Gaussian variable with unit variance. The propagator deforms the large-scale statistics when the scale l is reduced below the integral scale L. In the simple situation where no dissipative scale is taken into account, and where the propagator is supposed independent of large-scale statistics, one can write formally the PDF of the Eulerian velocity increments $\delta_l v = \sigma_L (l/L)^h \delta$ as [43]

$$p_{\delta_l v}(\delta_l v) = \int_{-\infty}^{\infty} \frac{1}{\sigma_L} \left(\frac{l}{L}\right)^{-h} \mathcal{P}_\delta \left[\frac{\delta_l v}{\sigma_L}\left(\frac{l}{L}\right)^{-h}\right] \mathcal{P}_h[h]\, dh, \tag{17}$$

where h is the Hölder exponent. We have notated $\mathcal{P}_\delta(\delta)$ and $\mathcal{P}_h(h)$ the probabilities of the independent random variables δ and h. The PDF $\mathcal{P}_h(h)$ depends only on the singularity spectrum $\mathcal{D}(h)$. See Ref. [43] for a detailed explanation.

We integrate numerically Eq. (17) to get the PDF of the increments $\delta_l v$, and then compute the KL divergence D_τ for several singularity spectra, either log-normal or log-Poisson.

Log-normal model: We varied the value of the log-cumulant c_1 and didn't observe any dependence of D_τ on c_1. On the other hand, varying c_2 strongly changes the convergence. Results are presented in Fig. 5(a). We observe and report in Fig. 5(b) that curves for different values of c_2 can be collapsed into a single curve when plotted as a function of $c_2 \ln(\tau/T) = c_2 \ln(l/L)$.

To understand this scaling behavior, we performed a saddle-node expansion of expression (17) in the log-normal case and obtained the following simplified expression for the PDF of

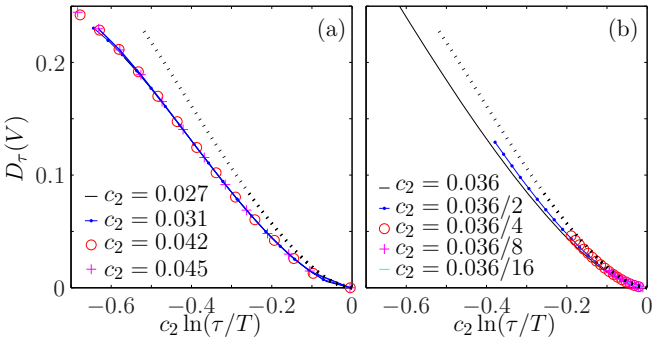

FIG. 6. Kullback-Leibler divergence D_τ as a function of $c_2 \ln(\tau/T)$ for the log-Poisson propagator model, for varying values of λ (a) and β (b). The dotted line represents the single curve obtained for the log-normal propagator [Fig. 5(b)].

the normalized increments $y = \delta_l v/\sigma_l$ at scale l:

$$p_y(y) = \frac{e^{\frac{3}{2}c_2 x}}{\sqrt{2\pi}} \frac{e^{-\frac{2W+W^2}{8c_2 x}}}{\sqrt{1+W}}, \tag{18}$$

where we have noted $x \equiv -\ln(l/L)$ the logarithmic scale, and W the value of the Lambert W-function of argument $2c_2 x y^2 e^{4c_2 x}$. Equation (18) is a non-Gaussian PDF which converges to the Gaussian PDF of variance σ_L^2 when $x \to 0$. From Eq. (18), the PDF of the increments depends only on $\ln(l/L) = \ln(\tau/T)$ and c_2 via the product $c_2 \ln(l/L)$. As a consequence, the entropy of the increments depends on the scale l as $c_2 \ln l/L$ only. This implies that the KL divergence D_τ for the log-normal process has the scaling observed in Fig. 5(b).

Log-Poisson model: We varied independently γ, λ, and β. We didn't observe any change of D_τ when γ was varied. This can be understood as γ changes only the value of c_1 [see Eq. (14)], which does not impact D_τ. Varying λ changes the convergence, as this amounts to change c_2 [see Eq. (15)], but we observe again that D_τ depends only on $c_2 \ln(\tau/T)$; see Fig. 6(a). This can be understood by noting that all log-cumulants are linear in λ; thus varying λ amounts to a change of c_2 while keeping higher order cumulants within the same ratio. On the other hand, varying β has more impact on the convergence, and the rescaling in $c_2 \ln(\tau/T)$ is then not perfect, albeit still relevant; see Fig. 6(b). This can be understood by noting that changing β changes not only c_2, but also the ratio of all higher order cumulants.

Comparison between models: The rescaling in $c_2 \ln(\tau/T)$, which absorbs most, if not all, the dependence of D_τ on c_2, allows a direct comparison of models. As can be seen in Fig. 6, all curves obtained with the log-Poisson propagator model clearly differs from the ones obtained with the log-normal propagator, especially for smaller scales. This probably results from the presence of higher order log-cumulants c_p, $p > 2$ in the log-Poisson propagator. As a consequence, whatever the choices of the propagators parameters, the KL divergence behaves very distinctly in the log-normal and log-Poisson models.

Comparison with turbulence data: Among open questions regarding statistical descriptions of Eulerian turbulence is the choice of a log-normal or log-Poisson modeling of its multifractal nature. We of course want to address this issue, and

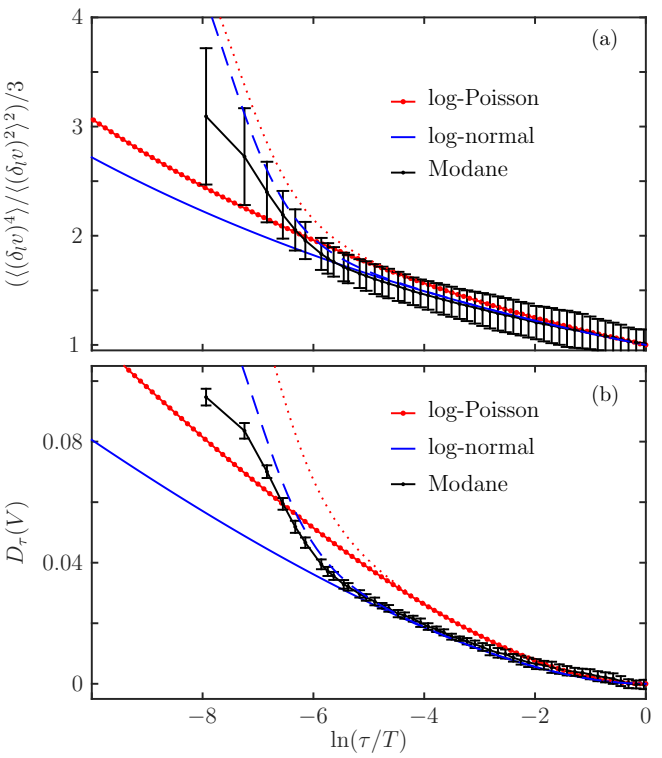

FIG. 7. Comparison of the two propagator models of turbulence [log-normal (continuous blue line) and log-Poisson (red dotted line)] with Modane experimental data (in black with error bars), as a function of $\ln(\tau/T)$: (a) normalized flatness, (b) KL divergence. The dashed (blue) and dotted (red) lines represent the modified models that take into account the dissipative range [43].

we explore both the flatness and the KL divergence to compare the two propagator models with experimental data in Fig. 7. In both models, parameters are set to the values acknowledged for turbulence (see Sec. IV A). For experimental data, we remove the bias from the KL divergence estimation by subtracting the small constant value that we measured for a fBm signal, see Fig. 4(b). As the c_2 value for turbulence is *a priori* unknown, we do not rescale the x axis with c_2. Let us remark though that the c_2 value we have used in the log-normal propagator ($c_2 = 0.025$) is exactly the one measured in experimental data, using multifractal analysis [43].

In the inertial range, although the flatness behaves differently for the two propagator models, the difference is small and remains within the error bars of the estimation performed on experimental data. On the contrary, when looking at the KL divergence, our results show a much better agreement of the log-normal model with the experimental data. Although this may be due to the very appropriate choice of c_2 in the log-normal model, the log-Poisson model does not allow such a choice and fixes all the log-cumulants [41]. As a consequence, we can state that the deformation of the experimental velocity increments PDF in the inertial range is better modeled by a multiplicative cascade with log-normal multipliers.

In the dissipative range, i.e., for smaller scales $\ln(\tau/T) \lesssim -5$, we observe a rapid increase of D_τ for the experimental data, which the two models (continuous lines in Fig. 7) fail to reproduce. This is expected, as both propagator models

were proposed to describe the inertial range only, and as such do not incorporate any modeling of the dissipative scales. To probe the dissipative range, we use the extension described in Ref. [43] and indicate the results for both propagators with dashed lines in Fig. 7. The rapid increase of intermittency in the dissipation range is captured by the flatness and the KL divergence. Although great care should be taken when commenting on the lowest accessible scales in the experimental data (mainly due to the acquisition process), we observe once again that the KL divergence indicates, much more clearly than the flatness does, that the log-normal propagator model is closer to the experimental observations.

V. DISCUSSION AND CONCLUSIONS

We have measured the Shannon entropy of the Eulerian turbulent velocity increments and studied its dependence on the scale. We have recovered three different behaviors in the integral, inertial, and dissipative domains, in perfect agreement with the classical analysis using, e.g., the power spectrum. In particular, in the inertial range, a scaling law for the entropy is observed, reminiscent of K41 theory, similar to what was earlier reported for another information theory quantity [36]. A closer look at the entropy, and especially a comparison with its Gaussian approximation, which takes into account only the variance of the signal, exactly as the PSD does, allows a much finer description and in particular a measure of intermittency, as introduced in KO62.

We have proposed a quantitative measure of intermittency. Although some quantities were already used as an intermittency coefficient, most, if not all, were ratios of structure functions [14], and as such, they were depending on the chosen ratio: flatness, hyper-flatness [10], or higher order ratios. We interpret intermittency as the distance from Gaussianity and measure it as D_τ, the Kullback-Leibler divergence between the complete PDF $p(\delta_\tau V)$ and its Gaussian approximation $p_G(\delta_\tau V)$; the first involves all the statistical moments, while the second one only depends on the variance. Our measure of intermittency, by comparing complete PDFs, takes into account all the moments of the distributions, which leaves no room for ambiguity on the choice of the moments.

We have checked the robustness of our approach by analyzing several experimental data sets, from two different experimental setups, and with varying Reynolds numbers.

The quantity D_τ is not only able to measure intermittency in turbulence, but also to discriminate very easily monofractal from multifractal processes. Furthermore, the evolution of D_τ with the scale depends on the process: this provides a much more precise characterization of the process than the bare set of log-cumulant values (c_1,c_2) given by a regular multifractal analysis. This may be exploited to discriminate log-Poisson from log-normal models of intermittency in turbulence.

We have investigated the dependence of D_τ on the log-cumulants. D_τ does not depend on c_1, and we have captured its dependence on c_2, and especially how it affects the convergence to 0 at large scales. Because D_τ appears to mainly depend on $c_2 \ln(\tau/T)$, we can state that the speed of the deformation of the PDF, starting from a Gaussian at large-scale L, depends on c_2. For a given scale l/L, or equivalently τ/T, the deformation of the PDF, and hence the intermittency, is an increasing function of c_2. Conversely, for a fixed value of c_2, the influence, or reminiscence, of the integral scale persists down to scales l/L smaller and smaller when c_2 is reduced. Because the typical c_2 of turbulence is small, the influence of the integral scale persists in the inertial domain, down to the dissipative domain, unless the Reynolds number tends to arbitrarily large values. We have shown that D_τ depends on higher order log-cumulants c_p, for $p > 2$, by looking at the special case of log-Poisson statistics (Fig. 6). The dependence seems weak, but is nevertheless present, and could be exploited.

Our measure of intermittency substantially differs from the existing measure involving the flatness. KL divergence gives a sharper contrast between propagator models; this is not surprising as KL divergence offers a complete perspective on the PDF and all its moments. In addition, the error bars of the KL divergence of experimental data are sufficiently small to allow a quantitative comparison of experiments with model predictions. This comparison was not instructive using previously existing tools. Our results show that KL divergence offers quantitative arguments in favor of a log-normal description of the propagator for modeling the distribution of Eulerian velocity increments across scales.

Although we have put a strong emphasis on turbulence, we want to point out that our approach is extremely general and should find successful applications in many other fields. It should prove particularly interesting for non-Gaussian processes, the most common in nature and society. Any multifractal process, or process that may be considered multifractal in some range of scales, can be analyzed with D_τ. The local intermittency measure that D_τ provides can be used to characterize the process at any scale.

ACKNOWLEDGMENTS

The authors wish to thank L. Chevillard for stimulating discussions. This work was supported by the Laboratoire d'Excellence (LabEx) iMUST (ANR-10-LABX-0064) of Université de Lyon, within the program "Investissements d'Avenir" (ANR-11-IDEX-0007) operated by the French National Research Agency (ANR).

[1] A. Feldmann, A. C. Gilbert, and W. Willinger, Data networks as cascades: Investigating the multifractal nature of Internet WAN traffic, SIGCOMM Comput. Commun. Rev. **28**, 42 (1998).

[2] R. Fontugne, P. Abry, K. Fukuda, D. Veitch, K. Cho, P. Borgnat, and H. Wendt, Scaling in internet traffic: A 14 year and 3 day longitudinal study, with multiscale analyses and random projections, IEEE/ACM Trans. Netw. **25**, 2152 (2017).

[3] R. E. Boulos, N. Tremblay, A. Arneodo, P. Borgnat, and B. Audit, Multi-scale structural community organisation of the human genome, BMC Bioinformatics **18**, 209 (2017).

[4] Y. Ahn, J. Bagrow, and S. Lehmann, Link communities reveal multiscale complexity in networks, Nature (London) **466**, 761 (2010).

[5] J. Bouchaud and M. Potters, *Theory of Financial Risk and Derivative Pricing: From Statistical Physics to Risk Management* (Cambridge University Press, Cambridge, 2003).

[6] L. Borland, J. P. Bouchaud, J. F. Muzy, and G. Zumbach, The dynamics of financial markets - Mandelbrot's multifractal cascades and beyond, arXiv:cond-mat/0501292 (2005).

[7] A. N. Kolmogorov, The local structure of turbulence incompressible viscous fluid for very large Reynolds number, Dokl. Akad. Nauk SSSR **30**, 299 (1941), reprinted in Proc. R. Soc. London A **434**, 9 (1991).

[8] A. N. Kolmogorov, On the degeneration of isotropic turbulence in an incompressible viscous fluid, Dokl. Akad. Nauk SSSR **31**, 538 (1941).

[9] A. N. Kolmogorov, Dissipation of energy in isotropic turbulence, Dokl. Akad. Nauk SSSR **32**, 19 (1941).

[10] F. Anselmet, Y. Gagne, E. J. Hopfinger, and R. A. Antonia, High-order velocity structure functions in turbulent shear flow, J. Fluid Mech. **140**, 63 (1984).

[11] A. N. Kolmogorov, A refinement of previous hypotheses concerning the local structure of turbulence in a viscous incompressible fluid at high Reynolds number, J. Fluid Mech. **13**, 82 (1962).

[12] A. M. Oboukhov, Some specific features of atmospheric turbulence, J. Fluid Mech. **13**, 77 (1962).

[13] U. Frisch and G. Parisi, On the singularity structure of fully developed turbulence, in *Turbulence and Predictability in Geophysical Fluid Dynamics and Climate Dynamics*, edited by M. Gil, R. Benzi, and G. Parisi (North-Holland, 1985), pp. 84–88.

[14] U. Frisch, *Turbulence: The Legacy of A. N. Kolmogorov* (Cambridge University Press, Cambridge, 1995).

[15] L. Chevillard, B. Castaing, and E. Lévêque, On the rapid increase of intermittency in the near-dissipation range of fully developed turbulence, Eur. Phys. J. B **45**, 561 (2005).

[16] C. E. Shannon, A mathematical theory of communication, Bell Sys. Tech. J. **27**, 379 (1948).

[17] S. M. Pincus and R. R. Viscarello, Approximate Entropy: A Regularity Measure for Fetal Heart Rate Analysis, Obstet. Gynecol. **79**, 249 (1992).

[18] A. Porta, S. Guzzetti, N. Montano, R. Furlan, M. Pagani, A. Malliani, and S. Cerutti, Entropy, entropy rate, and pattern classification as tools to typify complexity in short heart period variability series, IEEE Trans. Biomed. Eng. **48**, 1282 (2001).

[19] A. Porta, V. Bari, T. Bassani, A. Marchi, S. Tassin, M. Canesi, F. Barbic, and R. Furlan, Entropy-based complexity of the cardiovascular control in Parkinson disease: Comparison between binning and k-nearest-neighbor approaches, in *Proceedings of the 35th Annual International Conference of the IEEE Engineering in Medicine and Biology Society (EMBC)* (IEEE, New York, 2013).

[20] T. M. Brown, Information theory and the spectrum of isotropic turbulence, J. Phys. A **15**, 2285 (1982).

[21] K. Ikeda and K. Matsumoto, Information Theoretical Characterization of Turbulence, Phys. Rev. Lett. **62**, 2265 (1989).

[22] R. T. Cerbus and W. I. Goldburg, Information content of turbulence, Phys. Rev. E **88**, 053012 (2013).

[23] J. M. Horowitz and M. Esposito, Thermodynamics with Continuous Information Flow, Phys. Rev. X **4**, 031015 (2014).

[24] S. Kullback, *Information Theory and Statistics* (Dover Publications, New York, 1968).

[25] R. Stresing, J. Peinke, R. E. Seoud, and J. C. Vassilicos, Defining a New Class of Turbulent Flows, Phys. Rev. Lett. **104**, 194501 (2010).

[26] D. Qi and A. J. Majda, Predicting fat-tailed intermittent probability distributions in passive scalar turbulence with imperfect models through empirical information theory, Commun. Math. Sci. **14**, 1687 (2016).

[27] E. T. Jaynes, Information theory and statistical mechanics. I, Phys. Rev. **106**, 620 (1957).

[28] E. T. Jaynes, Information theory and statistical mechanics. II, Phys. Rev. **108**, 171 (1957).

[29] T. M. Cover and J. A. Thomas, *Elements of Information Theory* (John Wiley & Sons, Hoboken, NJ, 2006).

[30] J. D. Victor, Binless strategies for estimation of information from neural data, Phys. Rev. E **66**, 051903 (2002).

[31] L. F. Kozachenko and N. N. Leonenko, Sample estimate of entropy of a random vector, Probl. Peredachi Inf. **23**, 9 (1987); Problems Inform. Transmission **23**, 95 (1987).

[32] N. Leonenko, L. Pronzato, and V. Savani, A class of Rényi information estimators for multidimensional densities, Ann. Statist. **36**, 2153 (2008).

[33] J. Theiler, Spurious dimension from correlation algorithms applied to limited time-series data, Phys. Rev. A **34**, 2427 (1986).

[34] H. Kahalerras, Y. Malecot, Y. Gagne, and B. Castaing, Intermittency and Reynolds number, Phys. Fluids **10**, 910 (1998).

[35] O. Chanal, B. Chabaud, B. Castaing, and B. Hebral, Intermittency in a turbulent low temperature gaseous helium jet, Eur. Phys. J. B **17**, 309 (2000).

[36] C. Granero-Belinchón, S. G. Roux, and N. B. Garnier, Scaling of information in turbulence, Europhys. Lett. **115**, 58003 (2016).

[37] B. B. Mandelbrot and J. W. Van Ness, Fractional Brownian motions, fractional noises and applications, SIAM Rev. **10**, 422 (1968).

[38] E. Bacry, J. Delour, and J. F. Muzy, Multifractal random walk, Phys. Rev. E **64**, 026103 (2001).

[39] R. F. Leonarduzzi, Análisis multifractal basado en coeficientes ondita líderes: selección automática del rango de escalamiento, formalismo multifractal basado en p-líderes y aplicación a señales biomedicas, Ph.D. thesis, Universidad Nacional del Litoral, Santa Fe, Argentina, 2014.

[40] A. Arneodo, E. Bacry, and J. F. Muzy, Random cascades on wavelet dyadic trees, J. Math. Phys. **39**, 4142 (1998).

[41] Z. S. She and E Leveque, Universal Scaling Laws in Fully Developed Turbulence, Phys. Rev. Lett. **72**, 336 (1994).

[42] B. Castaing, Y. Gagne, and E. J. Hopfinger, Velocity probability density functions of higher Reynolds number turbulence, Physica D **46**, 177 (1990).

[43] L. Chevillard, B. Castaing, A. Arneodo, E. Leveque, J. F. Pinton, and S. G. Roux, A phenomenological theory of Eulerian and Lagrangian velocity fluctuations in turbulent flows, C. R. Phys. **13**, 899 (2012).

[44] J. Delour, J. F. Muzy, and A. Arnéodo, Intermittency of 1D velocity spatial profiles in turbulence: A magnitude cumulant analysis, Eur. Phys. J. B **23**, 243 (2001).

[45] H. Helgason, V. Pipiras, and P. Abry, Fast and exact synthesis of stationary multivariate Gaussian time series using circulant embedding, Signal Process. **91**, 1123 (2011).

[46] V. Venugopal, S. G. Roux, E. Foufoula-Georgiou, and A. Arneodo, Revisiting multifractality of high-resolution temporal rainfall using a wavelet-based formalism, Water Resour. Res. **42**, W06D14 (2006).